RESEARCH

Wave-Slope Soaring of the Brown Pelican

Ian A Stokes[1,2*†] and Andrew J Lucas[1,2]

Abstract

Background: From the laboratory at Scripps Institution of Oceanography, one can observe the brown pelican (*Pelecanus occidentalis*) traveling along the crests of near-shoaling waves just outside the surf zone. In this manner, the birds travel great distances without flapping, all the while a scant $\sim$ 30 cm off the ocean's surface. Here we derive a theoretical framework for assessing the energetic benefit of this behavior, "wave-slope soaring," in which an organism in flight takes advantage of updrafts caused by traveling ocean surface gravity waves.

Methods: The energy cost of steady, constant altitude flight is analyzed as a control. Potential flow theory is used to quantify the ocean wave-induced wind associated with near-shoaling, weakly nonlinear, shallow water ocean surface gravity waves. Using a regular expansion of the Stokes stream function and the Green's function for Laplace's equation in 2D with Dirichlet boundary conditions, we obtain integral expressions for the horizontal and vertical components of the wave-induced wind. The development of these relationships produces expressions for the components of the wave-induced wind in a frame of reference moving with the wave. Wave-slope soaring flight is then analyzed using an energetics-based approach for waves of typical ocean conditions (wave height of 1m, period of 10s) and the body plan of *P. occidentalis*.

Results: For pure ground effect flight, we calculate an upper bound mechanical advantage of $\sim$ 20 - 25% as compared with steady, level flight without ground effect. When wave-slope soaring is employed, we calculate an upper bound mechanical advantage of $\sim$ 50 - 60% as compared with steady, level flight without ground effect.

Conclusions: The theoretical development presented here suggests there are energy savings associated with wave-slope soaring. Individual brown pelicans may gain upwards of 50% mechanical advantage utilizing this mode of flight under typical ocean conditions, as compared to steady, level flight out of ground effect. Thus wave-slope soaring appears to provide a significant benefit to these highly mobile organisms that depend on patchy prey distribution over large home ranges.

Keywords: Soaring; Wave-Slope Soaring; Dynamic Soaring; Seabird; Pelican; Wave-Induced Wind; Soliton; Cost-Effective Flight; Ocean Surface Gravity Waves; Theoretical Model

Background

The goal of this work is to estimate the energy savings associated with wave-slope soaring flight. To accomplish this, we perform a theoretical study of the brown pelican practicing wave-slope soaring over near-shoaling coastal waves. Wave-slope soaring is a flight method used commonly by many seabirds [1], but few species exhibit such mastery of the skill as the brown pelican, *Pelecanus occidentalis*, Linnaeus, 1766. This mode of flight makes use of aerodynamic gains from ground effect and the localized updrafts driven by traveling ocean surface waves. "Ground effect" here refers to the reduction in aerodynamic drag associated with flight close to a fixed surface [2].

For a visual reference, we encourage the reader to imagine they are standing on the beach, a cliff, or

*Correspondence: istokes@eng.ucsd.edu
[1] Dept. of Mechanical and Aerospace Engineering, University of California, San Diego, 9500 Gilman Drive, La Jolla, CA 92037, USA
[2] Scripps Institution of Oceanography, University of California, San Diego, 8622 Kennel Way, La Jolla, CA 92037, USA
Full list of author information is available at the end of the article
†Primary Author

a fishing pier, observing the coastal ocean. From this perspective, one can observe pelicans gliding along the crests of waves just outside the surf zone, as the wave begins to shoal and steepen. When the wave breaks and begins to dissipate, the bird uses its forward along-crest momentum to gain altitude and steer out to sea. The process starts again offshore as the pelican glides down to catch the next wave, thereby continuing down the coast. Several hundred meters of along-coast distance can be covered in this way on each set of ocean waves that hit the coast.

This flying behavior is similar to a surfer cruising along the open face of a peeling wave. The mechanics of wave riding are well described by Edge [3] in his study of surfing. He notes that "The main objective of the surfer is to ride the wave at the point that will carry him in with the greatest stability and highest speed possible. The actual distance it is possible to travel directly toward shore is relatively short, if the breaking cycle of the wave itself is short ... If, instead of moving directly perpendicular to the wave front, the surfer moves in a path more parallel to the crest, the ride can be greatly extended." [3]

Long before humans began surfing, brown pelicans had already learned the technique of riding a wave 'down-crest' – that is, at an angle more or less parallel coastline – in order to extend their ride to several or many seconds. It does not at appear that this behavior is related to play, as it can be in dolphins and sea-lions [4]. Instead, since these birds are known to feed on patchy resources and thus must travel long distances, we hypothesize that wave-slope soaring is conducive to achieving energy efficient flight.

Physical study of the various means of soaring used by birds has remained a topic of active research for many years. The phenomenon of "dynamic soaring" by wandering albatrosses was introduced in the nineteenth century by Rayleigh [5]. In the late twentieth century, this theory was refined by Wilson [1], but it was not until the twenty-first century that Sachs [6] experimentally verified the energetic benefit associated with this practice. Dynamic soaring is a particular flight behavior wherein the bird may gain energy from the vertical wind shear at the base of the atmospheric boundary layer [5, 7, 6, 1]. Since these energy gains through bird behavior more than offset losses to drag, these birds can soar for days, weeks, or even months without flapping. The wandering albatross may even circle the globe without flapping its wings [7]. In this process, the birds are also able to "sail" upwind, in a manner comparable to the beating and tacking employed by the helmsman of a sailboat [8].

On a research cruise in the southern ocean, Richardson [7] studied the conditions under which dynamic soaring becomes a cost-effective method of flight for several species of albatross. It was found that when the winds are strong, dynamic soaring was preferred, regardless of sea surface conditions. When the winds were light, but surface conditions provided swell, wave-slope soaring became the albatross' preferred method of travel [7]. The energetics of wave-slope soaring, however, were not quantified in that study.

Richardson [7] also documented that in conditions of light wind and minimal surf, rather than flight via flapping, albatrosses simply sit on the ocean surface until the wind or waves return [7]. Thus there must be an energy benefit to both dynamic and wave-slope soaring flight, as albatrosses are reluctant to fly without one or the other. While dynamic soaring has been widely studied and shown to be cost-effective energetically, wave-slope soaring has not received much attention in the literature. Specifically, there is no mathematical formalism describing wave-slope soaring, and it has rarely been mentioned in the literature outside the studies by Wilson [1] and Richardson [7].

1 Methods

To formulate the dynamics of wave-slope soaring, we use a three-prong approach. First, the controls are developed in section 1.1 where we analyze the cost of steady, constant altitude pelican flight in the absence of ocean surface waves, both out of ground effect (section 1.1.2) and in ground effect (section 1.1.3). These two results provide a means to isolate the energy savings associated with the wave from the energy savings of ground effect alone, given the significant simplifying assumptions we have employed. Second, a description of the updrafts caused by near-shoaling waves is essential. In the air-sea interactions literature, any displacement of air caused by traveling waves is known as "wave-induced wind". The description of wave-induced wind is, in general, very complex due to the broad spectrum of ocean surface waves and the nonlinear wave-wave and wave-wind interactions that can take place [9]. Since wave-slope soaring behavior is seen in calm wind conditions, and appears to favor long-period, long-crested swells, we proceed with a simplified model to describe wave-induced wind in calm conditions just offshore of the depth at which shoaling causes strong nonlinearities in the wave form, and ultimately breaking (Section 1.2). To retain some of the nonlinearities intrinsic to near-shoaling waves, but allow the problem to be analytically tractable, we assume a waveform shape of the well-studied soliton [10]. This approach has been effective in modeling near-shoaling, shallow water, ocean surface gravity waves, and was shown to be reasonable in the region just outside of the surf zone, where nonlinear steepening begins [10]. This simplification, along with the assumption of no mean airflow, allows us to assume a well-attached, viscous boundary layer [11]. Accordingly, we use potential flow theory to model the vertical component of the wave-induced wind outside the boundary layer. Finally, the wave-induced wind model is combined with flight in ground effect to assess possible energy benefit of wave-slope soaring (Section 1.3).

Table 1 Average Brown Pelican Parameters [12].

Parameter	Symbol	Value
Mass	M	2.65 kg
Wingspan	b	2.10 m
Total Wing Area	S	0.45 m^2
Wing Loading	W/S	57.8 N/m^2
Aspect Ratio	A	9.8

1.1 Pelican Flight in Absence of Ocean Waves

1.1.1 Assumptions and Parameters

Throughout this section we assume inviscid, incompressible, irrotational flow with constant air density ρ. Accordingly, we will use the Kutta-Joukowski theorem to assess the lift and drag experienced by the bird. In

this analysis, we draw upon the framework presented by Rayner [2] to estimate the energy-cost of flight in and out of ground effect. Crucial data for this analysis are the physical characteristics of the brown pelican relevant to flight. Pennycuick [12] obtained the lift coefficient of the brown pelican in straight flight out of ground effect as $C_L = 0.72$. Pennycuick [12] also took measurements of various average brown pelican parameters which we will use, given in Table 1.

In a later study, Pennycuick et al [13] obtain an experimentally derived relation for the body drag coefficients of large waterfowl and raptors, C_D, as a function of Reynolds number. This relation is given as $C_D \approx 1.57 - 0.108 \ln(\mathrm{Re})$, and holds for waterfowl flight with Reynolds number on the range of 5×10^4 to 2×10^5.

Using characteristic velocity and length scales corresponding to the flow over a pelican's wing, we assess the associated Reynolds number. We calculate the standard mean chord $\bar{c}$ assuming a straight tapered wing using the average pelican measurements given by Pennycuick [12]. This calculation yields $\bar{c} = S/b = 0.21$ m. Measurements given by Pennycuick [12] were taken from a sufficiently large dataset such that the average values can be taken to represent the population reasonably well. Pennycuick [12] determined the average speed of a brown pelican in straight flight to be roughly 10 m/s, which we will use as the characteristic velocity u_c for the Reynolds number analysis.

Taking characteristic values as well as the density and viscosity of air at room temperature, we obtain a Reynolds number of roughly 150,000. Since this estimate of Reynolds number lies between 50,000 and 200,000, we are justified in using the approximate body drag coefficient via the relation given by Pennycuick et al [13], yielding $C_D \approx 0.28$.

1.1.2 Flight out of Ground Effect

To analyze cost benefits of flight in ground effect, we must first obtain a baseline comparison through analysis of the steady, constant altitude flight of a pelican in still air, out of ground effect. The reference coordinate system here is constructed such that $\hat{\mathbf{z}}$ represents the vertical unit vector and $\hat{\mathbf{x}}$ represents the horizontal unit vector. Rayner [2] provides a valuable reference detailing the aerodynamics of animal flight, both in and out of ground effect. It is shown that the magnitude of the total drag as a function of airspeed over-wing can be written as

$$D(u) = \frac{2}{\pi\rho}\left(\frac{Mg}{bu}\right)^2 + \frac{\rho S C_D u^2}{2}. \tag{1.1.1}$$

Furthermore, if we minimize the magnitude of total drag using airspeed u as the independent variable, we obtain an estimate for the magnitude of the minimum energy cost velocity (u_{mc}) as

$$u_{mc} = \sqrt{\frac{2Mg}{\rho b\sqrt{\pi S C_D}}}. \tag{1.1.2}$$

Using the values corresponding to the brown pelican as given in Table 1, the calculated drag coefficient of 0.28, and the density of air at sea level, we find that $u_{mc} = 5.7$ m/s for the brown pelican. The power output by the animal to overcome the drag force and maintain constant velocity is given by $P = \mathbf{D}\cdot\mathbf{u}$, where

u is the velocity of airflow over the wing in absence of any external wind influence. As **D** and **u** both act in $\hat{\mathbf{x}}$, we can simply multiply the magnitudes, yielding the following general expression for the required power output for flight out of ground effect (P_{oge}) as a function of velocity

$$P_{oge}(u) = \frac{2}{\pi\rho u} \cdot \left(\frac{Mg}{b}\right)^2 + \frac{\rho S C_D u^3}{2}. \qquad (1.1.3)$$

Here, the first term represents the power required to overcome the induced drag and the second represents the power required to overcome the profile drag. "Induced drag" here refers to the component of drag related to the angle of attack, while "profile drag" refers to the component of drag related to the shape of the body in flight. Using (1.1.3), we evaluate the minimum cost of flight out of ground effect, $P_{oge}(u_{mc})$. Again using the values corresponding to the brown pelican as given in Table 1 and the calculated drag coefficient of 0.28, we find

$$P_{oge}(u_{mc} = 5.7m/s) \approx 28.2\ W. \qquad (1.1.4)$$

Thus, using canonical values for an average brown pelican, a simplified force balance yields the result that steady, level flight out of ground effect requires roughly 30 W of continuous power input, even at the speed of maximum efficiency. This implies that steady level flight comes at significant energy cost to a pelican. Behavioral adaptations that increase efficiency would allow significant gains in foraging and traveling range.

To validate this estimate, we investigate measured flight cost of similar marine bird species, as precise measurement of the metabolic power input for brown pelican flight is not readily available in the literature. Ballance [14], in study of the red footed booby, a similar (though smaller) marine bird, found that it expends $\sim$ 20 W in gliding flight. Dolnik and Gavrilov [15] also studied the energy-cost of several marine bird species: it was found that for the mallard duck in flapping flight, the required power output is $\sim$ 44 W and for the great black-backed gull in flapping flight, the required power output is $\sim$ 36.3 W. Thus, our calculated value of $\sim$ 30 W for sustained flight of the brown pelican certainly provides a reasonable estimate. Though further experiment will be required to verify this figure, we will use this value as the primary control for this theoretical study.

1.1.3 Flight in Ground Effect

Flight in ground effect decreases the induced drag, which is commonly referred to as "induced drag savings." However, as the form of the flier is constant whether in or out of ground effect, the form drag remains unchanged [16, 2]. As Hainsworth [16] has measured the induced drag savings associated with brown pelican flight in ground effect, we can simply apply these percentages to the first term of (1.1.3) to estimate the total power required for ground effect flight.

Hainsworth [16] reports average brown pelican ground-effect flight height of 33 cm, with a standard deviation of 5 cm. The full data-set of measured flight height is reported to range from 24 to 45 cm, while gliding in ground effect. Induced drag savings associated with

Table 2 Mechanical Power Advantage for a Brown Pelican flying in Ground Effect

Variable	Min Val	Avg Val	Max Val
H (cm)	24	33	45
$P_{ge}(u_{mc})$ (W)	20.7	21.4	22.5
% Advantage	26.6	24.1	20.2

Values are given for flight at heights in the ground effect range as reported by Hainsworth [16] and minimum cost flight speed $u_{mc} = 5.7$ m/s.

these flight heights are estimated from theory to fall on the range of 41% to 58%, with average induced drag savings of 49%. These percentages correspond to flight heights of 24, 45, and 33 cm, respectively [16].

When we apply these induced drag savings to the theoretical total aerodynamic drag, we find the following results. For flight heights of 24, 33, and 45 cm, total mechanical power output required for flight is 20.7 W, 21.4 W, and 22.5 W, with percent mechanical advantages of 26.6%, 24.1%, and 20.2% respectively when compared to the 28.2 W required for flight out of groound effect. These results are displayed in Table 2. Rayner's lifting line theory for animal flight in ground-effect reports "a reduction in mechanical flight power of as much as 35%, compared with values for flight out of ground effect" [2]. Thus these values agree with [2], and will be used for our secondary control.

1.2 Airflow Induced by Near-Shoaling Waves

1.2.1 Background

As ocean waves translate, they induce airflow as a result of the no-penetration condition on a boundary, even in the case where there is no ambient wind. Fascinatingly, wave-induced wind might have been first reported in 1925 by Idrac [17] in his study of albatrosses, who noted that traveling ocean surface gravity waves can produce updrafts with vertical velocity in excess of 2 m/s at 8 meters height. It was noted as well that these updrafts effects can be felt up to 15 meters above the ocean surface [17]. Many experiments have been carried out to explore different aspects of wave-induced wind, with a focus on its impacts on the ocean and atmospheric boundary layers, and turbulence therein. These include both numerical (e.g. [18]) and observational studies (e.g. [19, 20, 21]). More recently, the upward transfer of momentum from ocean swell to the wind was experimentally verified by [22] in their experiment aboard the Scripps Institution of Oceanography's FLoating Instrumentation Platform (R/P FLIP). Using wave measurement apparatus and an extensive array of ultrasonic anemometers, Grare et al [22] were able to accurately measure the wave-induced components of the wind velocity for various wind-wave conditions. From this data, an empirical curve for wave-induced wind components scaled with surface orbital velocity as a function of height above the ocean scaled with wavenumber (r^2 of 0.76) was produced. As a validation of our model, we compare our theoretical prediction for the vertical component of the wave-induced wind to the respective empirical model provided by Grare et al [22]. This is further discussed in section 1.2.4 and shown in Figure 2

1.2.2 Model of Near-Shoaling Waves

To obtain an analytically tractable solution for the complicated real-world case of evolving and steepening nonlinear waves nearing the beach, we will assume our analysis applies only to the area just offshore of the surf-zone, where these shallow-water near-shoaling waves can be approximated as solitons [10]. Under the

soliton approximation, we take the waves to be governed by the Korteweg-de Vries (KdV) equation [10]. Neglecting surface tension, we begin with the dimensional traveling soliton solution,

$$\eta(x,t) = A\,\mathrm{sech}^2(kx - \omega t), \tag{1.2.1}$$

where

$$\begin{aligned} A &\equiv \frac{4}{3}\,k^2h^3, \\ \omega &\equiv k\sqrt{gh} - \frac{2}{3}\,k^3h^2\sqrt{gh}. \end{aligned} \tag{1.2.2}$$

We use the dispersion relation to write the wave's dimensional phase velocity (c) as

$$c = \sqrt{gh}\left[1 - \frac{2}{3}(kh)^2\right]. \tag{1.2.3}$$

Our definition for the amplitude in (1.2.2) can be used to eliminate k from (1.2.3), allowing us to write the phase velocity as a function of amplitude and depth,

$$c = \sqrt{gh}\left[1 - \frac{A}{2h}\right]. \tag{1.2.4}$$

We now use the dispersion relation and the definition of amplitude given in (1.2.2) to write an expression for the period as a function of amplitude and depth,

$$T = \frac{4\pi h}{\sqrt{3gA}\left(1 - \frac{A}{2h}\right)}. \tag{1.2.5}$$

This expression yields a quadratic equation for h as a function of T and A, solution of which can be written as

$$h = \frac{T\sqrt{3gA}}{8\pi} + \frac{1}{2}\sqrt{\frac{3gAT^2}{16\pi^2} - \frac{T\sqrt{3gA^3}}{2\pi}}. \tag{1.2.6}$$

The negative branch is omitted as it produces negative ocean depths which is unphysical. With equations 1.2.4 and 1.2.6, we have a framework for which if we are provided the amplitude and period of any ocean swell, we can calculate the phase velocity in the region where these incoming swells will act as weakly nonlinear solitary waves.

1.2.3 Boundary Layer Effects

Banner and Melville [11] argue that the viscous boundary layer at the air sea interface will not separate if a waveform maintains a smooth and steady shape. They propose that only upon the onset of shoaling will the boundary layer proceed to separate. In this case, the boundary layer will separate at the peak of the crest, resulting in a connected boundary layer on the front side of the wave and a detached boundary layer in the rear. This theory was confirmed by Reul et al [23], who show that for shoaling waves, the viscous boundary layer separates when a discontinuity in slope develops at the crest.

Here, we are working with a simplified model that involves a smooth waveform, and we will assume a viscosity-dominated, well attached boundary layer [11, 23]. Using typical values for ocean waves we see that $\mathrm{Re} \sim O(10^7)$, and $\mathrm{Ma} \ll 0.2$. With such a small Mach number we will continue to assume that compressible effects are negligible. However, as the Reynolds number is large it is evident that a turbu-

lent boundary layer must exist. As the aspect ratio of the wave is large and its surface is assumed to be smooth, we estimate the length scale of the boundary layer (δ) using the theory for turbulent boundary layers along a flat plate channel. For length and velocity scales corresponding to solitons resulting from typical ocean conditions as constructed in section 1.2.2, we calculate this boundary layer thickness to be of $O(1)$ cm.

Due to the length scale of a pelican and the fact that it cannot risk crashing, the bird flies at minimum heights of $\sim$ 25 centimeters above the surface [16]. Thus we neglect the boundary layer in calculations. Outside of the boundary layer, viscous effects are negligible and therefore we can assume inviscid flow in the regime relevant to wave-slope soaring.

1.2.4 Potential Flow over Solitary Waves

The wave-induced wind we describe is assumed to be inviscid, irrotational, and incompressible within our region of interest. With these assumptions and a well-connected boundary layer, it is appropriate to approximate the flow induced by the traveling solitary wave using potential flow theory. The goal of this section is to model potential flow over the soliton

$$\eta = A\ \mathrm{sech}^2(kx), \tag{1.2.7}$$

moving at phase speed c. We first boost to a frame of reference moving with the soliton such that $U_\infty = -c$, as shown in Figure 1. As we are assuming potential flow conditions, the system is governed by Laplace's equation for the stream function,

$$\Delta\psi = 0. \tag{1.2.8}$$

We can only impose the no penetration boundary condition

$$\left[\mathbf{u}\cdot\hat{\mathbf{n}} = 0\right]_{z=A\ \mathrm{sech}^2(kx)}. \tag{1.2.9}$$

We introduce the non-dimensional coordinates

$$\zeta = kz, \qquad \xi = kx. \tag{1.2.10}$$

From (1.2.2) we can write

$$Ak = \frac{4}{3}(kh)^3. \tag{1.2.11}$$

As the soliton was derived in the limit of $\lambda \gg h$, it follows that $kh \ll 1$. We will define another nondimensional coordinate $\epsilon \equiv Ak$ such that $\epsilon = \frac{4}{3}(kh)^3 \ll 1$. Thus, we can express the boundary in terms of nondimensional coordinates as

$$\zeta = \epsilon\ \mathrm{sech}^2(\xi). \tag{1.2.12}$$

Since $\epsilon \ll 1$ in the scaled geometry, to a first approximation we simply have to solve Laplace's equation in the upper half plane.

By the definition of the stream function, we have

$$u = \frac{\partial\psi}{\partial\zeta}, \qquad w = -\frac{\partial\psi}{\partial\xi}. \tag{1.2.13}$$

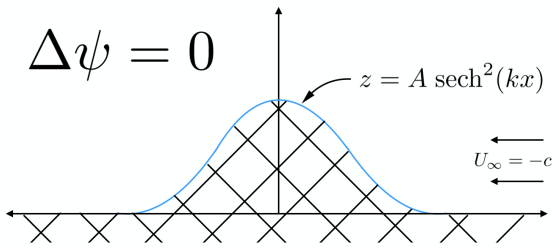

Figure 1 Schematic of the potential flow problem setup in the $x - z$ plane.

In terms of the stream function, the boundary condition (1.2.9) enforces that ψ must be constant everywhere on the sea surface. Integrating (1.2.13 a), using the condition that as $\xi \to \pm\infty$, $\psi \to -c\,\zeta$, and taking ψ to be constant on the sea surface gives the condition

$$\psi(\xi, \epsilon\ \mathrm{sech}^2\xi) = 0. \tag{1.2.14}$$

Now, as $\epsilon \ll 1$ we Taylor expand (1.2.14). This gives

$$\begin{aligned}\psi(\xi,0) + \epsilon\ \mathrm{sech}^2(\xi)\psi_\zeta(\xi,0) \\ + \frac{1}{2}\,\epsilon^2\mathrm{sech}^2(\xi)\psi_{\zeta\zeta}(\xi,0) + O(\epsilon^3) = 0,\end{aligned} \tag{1.2.15}$$

where subscripts denote partial derivatives. We now expand ψ in a regular expansion, yielding

$$\psi = \psi_0 + \epsilon\ \psi_1 + \epsilon^2\ \psi_2 + O(\epsilon^3), \tag{1.2.16}$$

where for all ψ_n with $n \in [0, \infty)$, $\Delta\psi_n = 0$. At $O(\epsilon^0)$, $\Delta\psi_0 = 0$. Integration yields

$$\psi_0 = -c\,\zeta. \tag{1.2.17}$$

Now from (1.2.15), we obtain

$$\begin{aligned}&\left[\epsilon\ \psi_1(\xi,0) + \epsilon^2\ \psi_2(\xi,0) + O(\epsilon^3)\right] \\ &+ \epsilon\ \mathrm{sech}^2(\xi)\left[-c + \epsilon\ \psi_{1,\zeta}(\xi,0) + O(\epsilon^2)\right] \\ &+ \frac{1}{2}\epsilon^2\mathrm{sech}^2(\xi)[0] + O(\epsilon^3) = 0.\end{aligned} \tag{1.2.18}$$

At $O(\epsilon^1)$,

$$\psi_1(\xi,0) = c\ \mathrm{sech}^2(\xi). \tag{1.2.19}$$

At $O(\epsilon^2)$,

$$\begin{aligned}\psi_2(\xi,0) + \mathrm{sech}^2(\xi)\psi_{1,\zeta}(\xi,0) \\ + \mathrm{sech}^2(\xi)\psi_{1,\zeta}(\xi,0) = 0.\end{aligned} \tag{1.2.20}$$

Using the Green's function for Laplace's equation in 2D with the Dirichlet boundary condition in (1.2.19), we obtain an expression for $\psi_1(\xi,\zeta)$ as

$$\psi_1(\xi,\zeta) = \frac{c}{\pi}\int_{-\infty}^{\infty} \frac{\zeta\ \mathrm{sech}^2(\xi')}{(\xi-\xi')^2 + \zeta^2}\,d\xi', \tag{1.2.21}$$

where ξ' is the variable of integration. This is an integral with no analytical solution. We remove the singularity by dividing the domain of integration at $\xi' = \xi$. Combined with (1.2.16), we can now obtain a full expression for ψ as

$$\begin{aligned}\psi = -c\zeta + \frac{Akc}{\pi}\int_0^{\infty} \frac{\zeta}{\xi'^2 + \zeta^2}\Big[\mathrm{sech}^2(\xi-\xi') \\ +\ \mathrm{sech}^2(\xi+\xi')\Big]d\xi' + O(\epsilon^2),\end{aligned} \tag{1.2.22}$$

where ξ' remains our variable of integration. This expression can now be evaluated numerically. Using (1.2.13 a), we can carry out the differentiation to ob-

tain an integral for the horizontal flow speed u in the frame of reference moving with the wave to the order of ϵ in terms of scaled coordinates as

$$u = -c + \frac{Akc}{\pi} \int_0^\infty \frac{\xi'^2 - \zeta^2}{(\xi'^2 + \zeta^2)^2} \Big[\mathrm{sech}^2(\xi - \xi') + \mathrm{sech}^2(\xi + \xi') \Big] \, d\xi' + O(\epsilon^2), \tag{1.2.23}$$

where we have substituted the definition of ϵ ($\epsilon \equiv Ak$) back into the expression. Similarly, we can use (1.2.13 b) to write an integral for the vertical flow speed w to $O(\epsilon)$ in terms of scaled coordinates as

$$w = \frac{2Akc}{\pi} \int_0^\infty \frac{\zeta}{\xi'^2 + \zeta^2} \Big[\mathrm{sech}^2(\xi - \xi')\tanh(\xi - \xi') + \mathrm{sech}^2(\xi + \xi')\tanh(\xi + \xi') \Big] \, d\xi' + O(\epsilon^2). \tag{1.2.24}$$

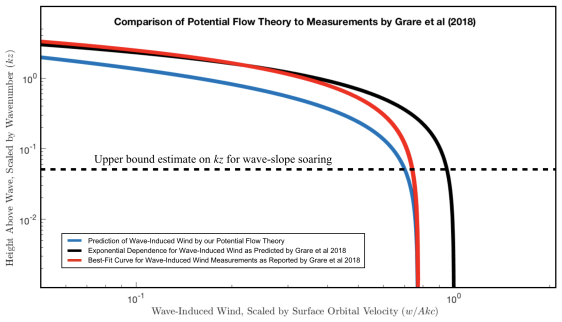

Figure 2 Wave-induced wind scaled with surface orbital velocity is shown on the x-axis and scaled height is shown on the y-axis in a log-log plot. In the region of wave-slope soaring, we see reasonable agreement with the best-fit curve for the vertical component of wave-induced wind, as reported by Grare et al [22]. This best-fit curve is given as

$$w/Akc = 0.85\Big[1 - 0.66 \cdot \exp\Big(-\Big|\frac{c}{u} - 1\Big|\Big)\Big]\exp(-0.83 \cdot kz),$$

with $r^2 = 0.76$. We see that near the wave, our model and the best-fit curve are in close agreement, while at greater heights above the wave, the best-fit curve trends more towards the exponential dependence that was predicted by Grare et al [22].

To validate our expression for wave-induced wind, we compare our predictions to the findings of Grare et al [22] (Fig. 2), using the vertical component of the wave-induced wind non-dimensionalized by surface orbital velocity (Akc), and the previously defined non-dimensional vertical height $\zeta = kz$. In our region of interest ($kz \leq 0.05$), we see good agreement with the measurements (Fig. 2; Grare et al [22]).

In order to evaluate the flow velocities, we need the wave number k. Using the linear dispersion relation, we obtain an expression for the wavenumber in terms of phase velocity and period as $k = 2\pi/cT$. (1.2.4) and (1.2.6) can be used to produce the phase velocity of our model wave in terms of amplitude and period. Following this analysis, the resultant phase velocity, wavenumber, and given amplitude can be inserted into (1.2.23) and (1.2.24) to produce the theoretical wave-induced wind in the near-shoaling regime relevant to wave-slope soaring.

1.3 Wave-Slope Soaring Flight

1.3.1 Assumptions and Coordinate System

We define coordinates such that $\hat{\mathbf{x}}$ is in the direction of wave propagation, $\hat{\mathbf{y}}$ is parallel to the wave front, and $\hat{\mathbf{z}}$ is in the vertical direction. A schematic of this coordinate system is shown in Figure 3. This enables us to make a few observations and assumptions. First we note that in order to gain benefit from the wave for extended periods of time, the bird must translate in $\hat{\mathbf{x}}$ so that its velocity in the direction of wave propagation

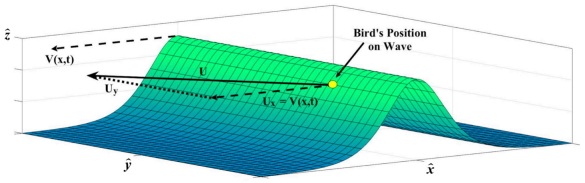

Figure 3 Coordinate system for the trajectories of a pelican in wave-slope soaring on a solitary wave.

(U_x) will match the phase velocity of the wave, $V(x,t)$. As stated above, we assume that the bird translates in $\hat{\mathbf{y}}$ so that the ocean depth under the bird remains constant. This results in soaring over a waveform that will remain constant in time in the pelican's frame of reference.

It is further assumed that the bird will fly at the optimal location in the space above the wave, and will remain at this location for the duration of soaring flight. All of these assumptions mean that the slope of the wave under the bird will remain constant. Hence the relevant wave-induced air flow is steady and irrotational in the bird's frame of reference. The phase velocity of the wave is constant so that $V(x,t) = c$. Using the formalism developed in section 1.2, with known swell period and amplitude we can determine the phase speed, c.

To a first approximation, we will consider the case where the bird is exactly level. From observation, this is commonly the case. Since we are assessing energy savings, we set the bird's net flight speed to the minimum-cost velocity, letting $U = u_{mc}$. Analysis at minimum cost-velocity also enables easier comparison to our controls of flight in and out of ground effect. It follows from section 1.2 that the optimal flight location is directly over the inflection point of the wave surface, where the slope is the steepest.

1.3.2 Energetics and Power of Wave-Slope Soaring

We will study this idealized case now under the assumptions stated above. We consider the mechanical energy balance of the system following Taylor et al [24]. The total energy of the system is given as

$$E = \frac{1}{2} M \mathbf{u}_{bird} \cdot \mathbf{u}_{bird} + M\mathbf{g} \cdot \mathbf{x}, \tag{1.3.1}$$

where $\mathbf{x}$ is the bird's inertial position and $\mathbf{u}_{bird}$ is the velocity of the airflow over the bird's wings. As we are interested in the required power output by the bird, we differentiate with respect to time. Taylor et al [24] show that the energy budget can be expressed as

$$\begin{aligned} \frac{dE}{dt} = &\left[M\frac{d^2\mathbf{x}}{dt^2} + M\mathbf{g} \right] \cdot \mathbf{u}_{bird} \\ &+ M\mathbf{g} \cdot \mathbf{u}_{wind} - M\mathbf{u}_{bird} \cdot \frac{d\mathbf{u}_{wind}}{dt}. \end{aligned} \tag{1.3.2}$$

We now evaluate and simplify this general expression for the case of steady, constant altitude wave-slope soaring on a soliton with no ambient wind to obtain

$$\frac{dE}{dt} = M\frac{d^2\mathbf{x}}{dt^2} \cdot \mathbf{u}_{bird} + Mgw(\mathbf{x}). \tag{1.3.3}$$

The first term on the right hand side corresponds to loss due to drag, while the second term corresponds to the benefit from positioning on the wave-induced updraft. The difference, dE/dt, corresponds to the required mechanical power output if the bird is to main-

tain flight at constant velocity and altitude. With the framework constructed in this paper, we have the tools to evaluate the two terms on the right hand side of (1.3.3) in order to estimate the percent mechanical advantage associated with wave-slope soaring flight.

As the wavelength is large compared to the wingspan of the bird and the wave slope is small, we assume the same flight heights as observed by Hainsworth [16] for standard ground-effect flight. Carrying on with our previous assertion that the bird will fly at minimum-cost velocity in ground effect, the loss due to drag will be unchanged from that calculated in section 1.1.3.

For the x coordinate of the bird's center of mass (x_b), we find the point of maximum slope associated with the waveform developed in section 1.2.2. For the z coordinate of the bird's center of mass (z_b), we use the free surface elevation at this point of maximum slope and add the ground-effect flight heights [16]. Because of the angle that the bird must fly in order to match its velocity in the direction of wave propagation to the phase velocity of the wave, we ignore variation of the wave-induced wind over the wingspan of the bird. This justifies the use of a single value for w in (1.3.3). Accordingly, we calculate w from (1.2.24) using the coordinates (x_b, z_b) and parameters corresponding to typical ocean conditions (dominant swell period of ten seconds with a wave height of one meter).

With these ingredients, we use the energy budget in (1.3.3) to calculate the difference between the magnitudes of drag loss and updraft benefit (dE/dt). This value is inferred as the power output required for flight in wave-slope soaring, and the associated mechanical advantage percentages are calculated. These results are displayed in Table 3.

Table 3 Mechanical advantage for ground effect and wave-slope soaring relative to flight out of ground effect.

H	∞	24_{ge}	33_{ge}	45_{ge}	24_{ws}	33_{ws}	45_{ws}
P	28	20.7	21.4	22.5	10.3	11.5	13.4
%	0	26.6	24.1	20.2	63.5	59.2	52.5

Row 1: Flight heights (cm) correspond to the minimum and average ground effect flight heights as measured by Hainsworth [16]. Row 2: Required power output in Watts for a pelican to remain in steady, level flight out of ground effect, in standard ground effect, and in wave-slope soaring. Row 3: Mechanical advantages gained over flight out of ground effect for each respective case.

2 Results

From our control, we find that steady, constant altitude pelican flight out of ground effect requires a power output by the bird of $\sim$ 30 Watts. For consistency with Hainsworth [16], we consider ground effect flight at heights of 24, 33, and 45 centimeters. These heights result in a required mechanical power output by the bird of 20.7 W, 21.4 W, and 22.5 W, with 26.6%, 24.1%, and 20.2% mechanical advantage in each case, respectively, from ground effect. In the case of wave-slope soaring, where ground effect is enhanced by the updraft velocity of the irrotational flow over a wave of 1 meter height at 10 second period, we estimate a large increase in energy savings. For constant speed flight, wave-slope soaring lessens the required mechanical power output to 10-15 W, or a 50-60 % savings over steady level flight out of ground effect (3).

3 Discussion

For typical ocean conditions and a reasonable soaring height, we find the wave-slope soaring mode of flight to provide $\sim$ 50-60% mechanical advantage over flight out of ground effect. This provides a significant incen-

tive for pelicans to use the practice, especially considering the mechanical advantage of ground effect alone is only about 20-25%. Given that larger waves produce stronger updrafts, it is likely that for larger swells, wave-slope soaring could provide nearly all of the energy required to maintain constant altitude flight.

There are several limitations of the theory presented here. First, we used the simplifying assumption of the weakly nonlinear solitary waveform. In reality, when observing pelicans employing wave-slope soaring, it is common for them to soar well into the surf zone, where nonlinearities become progressively stronger. In this regime, it becomes unreasonable to approximate the waveform as a soliton, and a more elaborate theory or numerical simulation would need to be employed.

Since nonlinear steepening should increase the vertical component of the wave-induced wind, the solitary wave assumption provides us a lower bound on the benefit of wave-slope soaring. To fully develop this theory we need to account for the time evolution of the system. This would involve tracking the evolution of the wave form from the solitary-like regime all the way to the point of breaking. We have omitted time-evolution in this work in order to obtain an analytically tractable solution, but nonetheless it would be interesting to see how the mechanical advantage changes as the wave tracks towards shoaling, via appropriate computational fluid dynamics simulation.

The assumption of no mean airflow in our model is a significant simplification. Our solution is framed around the benefit of vertical flow in the atmosphere perturbed by a travelling wave, which would be significantly altered as wind speeds increase and the turbulent boundary layer tends toward separation between wave-crests. In regions with strong winds, like the Southern Ocean, wave-slope soaring in albatross is only observed during rare calm periods [7]. This suggests that as the boundary layer becomes increasingly turbulent, dynamic soaring is a more effective strategy. A separated, turbulent boundary layer may be less amenable to wave-slope soaring since updrafts associated with traveling waves may be reduced in magnitude or lose coherence along the wave crest (the direction of travel). Increased winds also of course lead to increasingly confused seas, which may complicate the spatial and temporal patterns of the wave-induced wind. Much like surfing in humans, perhaps wave-slope soaring is particularly effective with long-period swell, calm winds, and a glassy, smooth sea-surface.

Pelicans display several behaviors that minimize the energetic cost of flight. The most well-known is formation flight. Hainsworth [25] found that for Canadian geese flying in formation, induced drag is reduced by roughly 30-40%. In a later study of the brown pelican [16], exact drag savings associated with formation flight were unclear due to high variability in the positioning among the squadron, but it was surmised that formation flight provides savings on similar order to that found for Canadian geese. This hypothesis is rooted in the similar size and aspect ratio of the birds' form, as well as a tendency of brown pelicans to fly in formation. It is in fact common to observe brown pelicans using formation flight in conjunction with wave-slope soaring. We hypothesize that wave-slope soaring

in formation adds an additional cost benefit to that already inherent in wave-slope soaring, though theoretical description of this coupled phenomena is left for future research.

4 Conclusions

The theoretical work presented suggest that brown pelicans could gain upwards of 50% mechanical advantage utilizing wave-slope soaring under typical ocean conditions, as compared to steady, level flight out of ground effect. Although there must be some risk associated with flying at a relatively high speed very close to an undulating and evolving surface, the benefit in terms of efficiency, and the predictability of the shoaling waves apparently favors the behavior. Riding of shoaling and breaking waves has been documented in several species of marine mammals, wherein it is assumed that the activity represents play [4]. Brown pelicans, on the other hand, may be unique in their ability to leverage wave-riding for travel, since flight allows them to connect a set of multiple shoaling waves in sequence. This allows continuous wave-riding for periods of minutes, and may account for travel of kilometers up or down the coast. Cost-effective travel resulting from wave-slope soaring behavior may have an important impact on the foraging range and foraging strategy of these ecologically important and magnificent creatures.

Declarations

Dedication

This article is dedicated to the late Ken Melville, of Scripps Institution of Oceanography, who's life's work made this research possible.

Ethics approval and consent to participate

No pelicans were harmed or harassed in production of the theoretical study presented in this work.

Consent for publication

Not applicable.

Availability of data and material

Not applicable.

Competing interests

The authors declare that they have no competing interests.

Funding

AJL gratefully acknowledges the Office of Naval Research (ONR) Young Investigator Program Fellowship (ONR N00014-17-1-2987) for supporting this effort. IAS was supported by ONR grant (ONR N00014-17-1-2112)

Author's contributions

IAS developed the mathematical formalism central to the manuscript. Both authors contributed to framing the problem, developing the approach presented here, and writing the manuscript. This manuscript began as a Masters thesis for IAS at the Department of Mechanical and Aerospace Engineering at the University of California, San Diego.

Acknowledgements

We would like to thank Benjamin Monreal of Case Western Reserve University for introducing the us to the problem, as he observed pelicans wave-slope soaring during his years at the University of California, Santa Barbara, and noted that no proper theoretical solution existed in the literature. After reviewing the initial sketch up of the problem, Anthony Zee of the Kavli Institute of Theoretical Physics at the University of California, Santa Barbara expressed interest, encouraging us to extend the theory and analysis into a manuscript. Stefan Llewellyn-Smith and Bill Young at the University of California, San Diego, aided in the refinement of the mathematical methods used in this work. We further thank Stefan Llewellyn-Smith for providing useful feedback on the manuscript. Finally, we dedicate this manuscript to the late Ken Melville of Scripps Institution of Oceanography–a pioneer in the study ocean surface waves and air-sea interactions–for his suggestion on use of the soliton formalism to represent near-shoaling, shallow water, ocean surface gravity waves.

Author details

[1] Dept. of Mechanical and Aerospace Engineering, University of California, San Diego, 9500 Gilman Drive, La Jolla, CA 92037, USA. [2] Scripps Institution of Oceanography, University of California, San Diego, 8622 Kennel Way, La Jolla, CA 92037, USA.

References

1. Wilson J. Sweeping flight and soaring by albatrosses. Nature. 1975;257(5524):307–308.
2. Rayner JM. On the aerodynamics of animal flight in ground effect. Philosophical Transactions of the Royal Society of London Series B: Biological Sciences. 1991;334(1269):119–128.
3. Edge R. Surf physics. The Physics Teacher. 2001;39(5):272–277.
4. Paulos RD, Trone M, Kuczaj II SA. Play in wild and captive cetaceans. International Journal of Comparative Psychology. 2010;23(4).
5. Rayleigh L. The soaring of birds. Nature. 1883;27(701):534–535.
6. Sachs G, Traugott J, Nesterova A, Bonadonna F. Experimental verification of dynamic soaring in albatrosses. Journal of Experimental Biology. 2013;216(22):4222–4232.
7. Richardson PL. How do albatrosses fly around the world without flapping their wings? Progress in Oceanography. 2011;88(1-4):46–58.
8. Richardson PL, Wakefield ED, Phillips RA. Flight speed and performance of the wandering albatross with respect to wind. Movement ecology. 2018;6(1):1–15.
9. Semedo A, Saetra Ø, Rutgersson A, Kahma KK, Pettersson H. Wave-induced wind in the marine boundary layer. Journal of the Atmospheric Sciences. 2009;66(8):2256–2271.
10. Barthélemy E. Nonlinear shallow water theories for coastal waves. Surveys in Geophysics. 2004;25(3-4):315–337.
11. Banner ML, Melville WK. On the separation of air flow over water waves. Journal of fluid mechanics. 1976;77(4):825–842.

12. Pennycuick CJ. Thermal soaring compared in three dissimilar tropical bird species, Fregata magnificens, Pelecanus occidentals and Coragyps atratus. Journal of Experimental Biology. 1983;102(1):307–325.
13. Pennycuick C, Obrecht HH, Fuller MR. Empirical estimates of body drag of large waterfowl and raptors. Journal of Experimental Biology. 1988;135(1):253–264.
14. Ballance LT. Flight energetics of free-ranging red-footed boobies (Sula sula). Physiological Zoology. 1995;68(5):887–914.
15. Dolnik V, Gavrilov V. Energy metabolism during flight of some passerines. Bird Migrations: Ecological and Physiological Factors Wiley, New York. 1973;p. 288–296.
16. Hainsworth FR. Induced drag savings from ground effect and formation flight in brown pelicans. Journal of Experimental Biology. 1988;135(1):431–444.
17. Idrac P. Experimental study of the "soaring" of albatrosses. Nature. 1925;115(2893):532–532.
18. Sullivan PP, Edson JB, Hristov T, McWilliams JC. Large-eddy simulations and observations of atmospheric marine boundary layers above nonequilibrium surface waves. Journal of the Atmospheric Sciences. 2008;65(4):1225–1245.
19. Högström U, Smedman A, Sahleé E, Drennan W, Kahma K, Pettersson H, et al. The atmospheric boundary layer during swell: A field study and interpretation of the turbulent kinetic energy budget for high wave ages. Journal of the atmospheric sciences. 2009;66(9):2764–2779.
20. Smedman A, Högström U, Sahlée E, Drennan W, Kahma K, Pettersson H, et al. Observational study of marine atmospheric boundary layer characteristics during swell. Journal of the atmospheric sciences. 2009;66(9):2747–2763.
21. Soloviev YP, Kudryavtsev V. Wind-speed undulations over swell: Field experiment and interpretation. Boundary-layer meteorology. 2010;136(3):341–363.
22. Grare L, Lenain L, Melville WK. Vertical profiles of the wave-induced airflow above ocean surface waves. Journal of Physical Oceanography. 2018;48(12):2901–2922.
23. Reul N, Branger H, Giovanangeli JP. Air flow separation over unsteady breaking waves. Physics of Fluids. 1999;11(7):1959–1961.
24. Taylor GK, Reynolds KV, Thomas AL. Soaring energetics and glide performance in a moving atmosphere. Philosophical Transactions of the Royal Society B: Biological Sciences. 2016;371(1704):20150398.
25. Hainsworth FR. Precision and dynamics of positioning by Canada geese flying in formation. Journal of Experimental Biology. 1987;128(1):445–462.